Hybrid Organometallic and Enzymatic Tandem Catalysis for Oxyfunctionalisation Reactions

Domestici, Chiara; Wu, Yinqi; Hilberath, Thomas; Alcalde, Miguel; Hollmann, Frank; Macchioni, Alceo

DOI
10.1002/cctc.202201623

Publication date
2023

Document Version
Final published version

Published in
ChemCatChem

Chemistry Europe
European Chemical Societies Publishing

WILEY VCH

Excellence in Chemistry Research

Announcing our new flagship journal

- Gold Open Access
- Publishing charges waived
- Preprints welcome
- Edited by active scientists

Meet the Editors of *ChemistryEurope*

Luisa De Cola
Università degli Studi di Milano Statale, Italy

Ive Hermans
University of Wisconsin-Madison, USA

Ken Tanaka
Tokyo Institute of Technology, Japan

ChemCatChem

Research Article
doi.org/10.1002/cctc.202201623

Chemistry Europe
European Chemical Societies Publishing

www.chemcatchem.org

Hybrid Organometallic and Enzymatic Tandem Catalysis for Oxyfunctionalisation Reactions

Chiara Domestici,[a] Yinqi Wu,[b] Thomas Hilberath,[b] Miguel Alcalde,[c] Frank Hollmann,*[b] and Alceo Macchioni*[a]

Unspecific peroxygenases (UPOs) are promising biocatalysts for oxyfunctionalisation reactions, owing to their simplicity of handling, stability and robustness. A limitation of using UPOs on a large scale is their deactivation in the presence of even rather modest concentrations of H_2O_2, requiring a constant and controlled supply of low amount of H_2O_2. Herein, we report an organometallic complex [Cp*Ir(pica)NO_3] {pica = picolinamidate = κ^2-pyridine-2-carboxamide ion (−1)} **1** capable of efficiently regenerating $FMNH_2$ from FMN (TOF = 350 h^{-1}, 298 K), driven by NaHCOO; $FMNH_2$, in turn, spontaneously reacts with O_2 leading to H_2O_2. After having studied the compatibility of **1** with the UPO from *Agrocybe aegerita* (r*Aae*UPO PaDa-I) and individuated the best experimental conditions, we applied such a hybrid catalytic tandem in some hydroxylation, epoxidation and sulfoxidation reactions. Best performances were obtained by using a **1**/r*Aae*UPO molar ratio of 50. TONs for the biocatalyst of up to 18933 were obtained for the transformation of ethylbenzene derivatives into (*R*)-1-phenylethanols (ee > 99%). **1**/r*Aae*UPO was found to oxidise also *cis*-methyl styrene (TON = 13488), leading exclusively (1*R*,2*S*)-*cis*-methyl styrene oxide (ee > 99%), cyclohexane (TON = 1634) and thioanisole (TON = 1369).

Introduction

The biocatalytic insertion of oxygen into non-activated organic molecules is attracting an increasing interest in pharmaceutical and industrial chemistry.[1] Particularly, enzyme-mediated oxyfunctionalisation reactions, such as hydroxylations or epoxidations, often reach high regio- and enantioselectivity providing alternative routes to the challenging conventional chemical methods. In this context, heme-containing P450 monooxygenases are widely utilised. They form the active oxyferryl-heme species via reductive activation of molecular oxygen.[2] Nevertheless, this pathway poses several difficulties such as dependence on costly nicotinamide cofactors, intricate electron transport chains as well as the so-called *Oxygen Dilemma*.[3] Some aspects may be solved through protein engineering while others are intrinsically linked to the enzymes' catalytic mechanisms. Fe-monooxygenases depend on single electron transfer processes, thus mediator species, such as ferredoxins and flavodoxins flavins are necessary to convert the hydride provided by NAD(P)H into two successive single electron transfer events to reduce the heme-iron. However, reduced mediators are radical species, and they can direct transfer electrons to dissolved atmospheric oxygen. For NAD(P)H the reaction with O_2 is spin-forbidden, conversely for ferredoxins or flavins it occurs rapidly. Hence, a significant proportion of the reducing equivalents provided by NAD(P)H can get lost in a wasteful uncoupling reaction with O_2, which leads to H_2O_2 eventually.[3] This hampers the large-scale usage of P450s.

Besides P450s, fungal unspecific peroxygenases (UPOs) have been recently exploited as selective oxyfunctionalisation biocatalysts.[4] The first unspecific peroxygenase isolated from the edible mushroom *Agrocybe aegerita* (*Aae*UPO, E.C. 1.11.2.1) was reported by Ullrich *et al.* in 2004.[5] Particularly, its evolved, recombinant variant (r*Aae*UPO PaDa-I)[6] has found considerable interest in the past years. Both enzyme classes utilise an oxyferryl heme as oxygenation species (compound I), however UPOs require only hydrogen peroxide that acts both as final electron acceptor and oxygen source. Thus, compared to P450s, UPOs exhibit a significantly simpler molecular architecture and regeneration scheme enabling the access to the same wide array of reactions and products.[4] Particularly, UPOs are able to catalyse the insertions of oxygen into non-activated aliphatic and aromatic C–H bonds and are considered the *Swiss Army Knife* of oxyfunctionalisation chemistry, thanks to the huge portfolio of reactions that they can mediate. Consequently, UPOs are emerging as a promising alternative to the estab-

[a] *C. Domestici, Prof. Dr. A. Macchioni*
Department of Chemistry, Biology and Biotechnology
University of Perugia and CIRCC
Via Elce di Sotto, 8
06123 Perugia (Italy)
E-mail: alceo.macchioni@unipg.it
Homepage: https://www.unipg.it/personale/alceo.macchioni
[b] *Y. Wu, Dr. T. Hilberath, Prof. Dr. F. Hollmann*
Department of Biotechnology
Delft University of Technology
Van der Maasweg 9
2629HZ Delft (The Netherlands)
E-mail: f.hollmann@tudelft.nl
Homepage: https://www.tudelft.nl/tnw/over-faculteit/afdelingen/biotechnology/research-sections/biocatalysis
[c] *Prof. Dr. M. Alcalde*
Department of Biocatalysis
Institute of Catalysis, CSIC
C/Marie Curie 2
28049 Madrid (Spain)

Supporting information for this article is available on the WWW under https://doi.org/10.1002/cctc.202201623

lished P450s. However, the H_2O_2-dependence of UPOs also bears the challenges of irreversible oxidative enzymatic inactivation.[7] Thus, continuous low-level supply or *in situ* generation of hydrogen peroxide (H_2O_2) is essential for the stability of peroxygenases.[8] To date enzymatic,[9] photocatalytic,[10] electrochemical,[11] transition metal catalysis-based[12] and 'miscellaneous'[13] *in situ* H_2O_2 generation approaches have been reported. Among the transition metal-based regeneration methods, Schmid and coworkers have reported the organometallic complex $[Cp^*Rh(bpy)(H_2O)]^{2+}$ for the production of H_2O_2 from formate, molecular oxygen and FAD as co-catalyst.[12b] Furthermore, $[Cp^*Rh(bpy)(H_2O)]^{2+}$ was coupled to cytochrome C in order to catalyse thioanisol sulfoxidation. Already under non-optimised reaction conditions, rhodium-based *in situ* H_2O_2 generation strategy has shown to be preferable than stoichiometric hydrogen peroxide usage.

A class of organometallic compounds potentially exploitable for H_2O_2 supply from formate, molecular oxygen and FMN as co-catalyst is constituted by Cp* iridium pyridincarboxyamidate complexes. They are extremely stable, water-soluble, and already used successfully as catalysts for hydrogenation reactions[14] with several reducing agents[15] in absence of any additives[16] and even in cellular media.[17] Moreover, they act as efficient catalysts for formic acid dehydrogenation,[15a,18] water oxidation, reductive amination of ketones,[19] hydrogenolysis of halosilanes,[20] and hydrogen peroxide generation[21] and they also exhibited good performance as antimicrobial and anti-cancer agents.[22]

Herein, we show that the organometallic complex $[Cp^*Ir(pica)NO_3]$ {pica = picolinamidate = κ^2-pyridine-2-carboxamide ion (−1)} **1** (Figure 1) is indeed a good catalyst for the H_2O_2-regeneration using simple flavin mononucleotide as co-catalyst and formate as hydride source. Furthermore, we disclose a chemoenzymatic tandem combining **1** with r*Aae*UPO to catalyse oxyfunctionalisation reactions. The feasibility of the proposed chemoenzymatic tandem is demonstrated by the wide portfolio of the reactions it can perform, including aromatic and (cyclo)aliphatic hydroxylation, epoxidation and sulfoxidation.

Results and Discussion

1 was synthesised following a modified literature procedure[15b] by the reaction of $[Cp^*Ir(H_2O)_3](NO_3)_2$ and pica in methanol, in the presence of 1 equivalent of KOH. **1** was characterised in solution by means of ^1H and ^{13}C NMR spectroscopy (Supporting Information).

Complex **1** was tested as possible catalyst in the reduction of FMN driven by formate [Equation (1)], following the progress of the reaction by means of a UV-Vis spectrophotometer. Particularly, the intensity of the band at 445 nm, diagnostic of FMN, was monitored (Figure S4).

$$FMN + HCOONa + H_3O^+ \rightarrow FMNH_2{}^*CO_2 + Na^+ + H_2O \quad (1)$$

All tests were performed under anaerobic conditions to avoid the spontaneous oxidation of $FMNH_2$ with atmospheric O_2 [Equation (2)], which might lead to an underestimation of the catalytic activity.

$$FMNH_2 + O_2 \rightarrow FMN + H_2O_2 \quad (2)$$

Indeed **1** proved to be and efficient catalyst for reaction (1), always leading to complete consumption of FMN, with a TOF of 350 h^{-1} (298 K, [FMN] = 0.1 mM, [HCOONa] = 200 mM, Table S1). The latter was found to be reasonably constant when **1** concentration was changed, suggesting a first-order dependence on catalyst concentration (Table S1 and Figure S5).

The performance of complex **1** compares well with that of $[Cp^*Rh(bpy)(H_2O)]^{2+}$ catalysing FMN and FAD reduction with TOF of 74.3 h^{-1} (at 310 K and [HCOONa] = 150 mM) and 28.4 h^{-1} (at 303 K; $[Cp^*Rh(bpy)(H_2O)]^{2+}$ = 0.025 mM; [FAD] = 1 mM and [HCOONa] = 500 mM), respectively.[23] It is worth mentioning that, to best of our knowledge, only one other Ir complex capable of reducing FMN has been reported in literature,[24] utilising H_2 instead of $HCOO^-$ to *in situ* generate the Ir–H reducing moiety.

As mentioned above, $FMNH_2$ in presence of atmospheric oxygen spontaneously oxidises to produce hydrogen peroxide (equation 2), thus indicating the possibility of producing H_2O_2 by the **1**-catalysed regeneration of the cofactor $FMNH_2$, driven by HCOONa (Scheme 1). As a matter of fact, a solution of **1** (0.025 mM), HCOONa (200 mM), and FMN (0.1 mM) in phosphate buffer (400 mM, pH 7), under aerobic conditions, generates hydrogen peroxide (> 100 mg/L after 1 h), as semi-quantitatively determined by QUANTOFIX®-Peroxide test sticks. This makes it possible, in principle, to supply a continuous low-level of hydrogen peroxide to the recombinant evolved peroxygenase from *Agrocybe aegerita* (r*Aae*UPO PaDa-I) for some oxyfunctionalisation reactions, assuming that for every

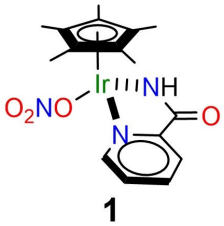

1

Figure 1. Sketch of $[Cp^*Ir(pica)NO_3]$ (**1**).

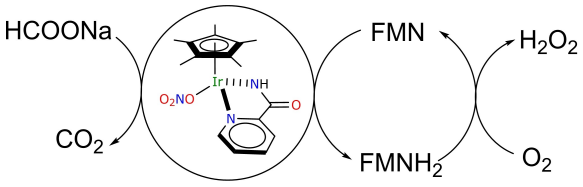

Scheme 1. *In situ* production of H_2O_2 by coupling the regeneration of $FMNH_2$ catalysed by $[Cp^*Ir(pica)NO_3]$, using formate as hydride source, with the spontaneous reaction of $FMNH_2$ under aerobic conditions.

equivalent of reduced FMN an equivalent of hydrogen peroxide is produced.

Before testing the **1**/r*Aae*UPO tandem in oxyfunctionalisation reaction, a battery of experiments was performed to investigate whether **1** and r*Aae*UPO undergo mutual inhibition. Previous studies have revealed that nucleophilic amino acid residues such as histidine or cysteine can coordinate to transition metal centres resulting in a mutual inhibition of both, the enzymes and the metal catalysts.[25] It is worth mentioning here that both, **1** and r*Aae*UPO are intrinsically stable under the given experimental conditions.[15,26] Catalyst **1** can be used even under acid and strong oxidising condition, despite its stability is somewhat reduced.[18c] Incubation of either of **1** and r*Aae*UPO alone in buffer resulted in no significant reduction of their catalytic activity over several days. In a first set of experiments the residual activity of **1** as $FMNH_2$ regeneration catalyst (reaction 1), in the presence of purified r*Aae*UPO in different molar ratios (50, 100 and 500) and different incubation times (1, 5 and 24 h) (Figure 2a and Table S2) was explored. The degree of **1**-inhibition correlated both with the **1**/r*Aae*UPO molar ratio and incubation time. As shown in Figure 2a, the tandem system was severely inhibited when **1**/r*Aae*UPO was equal to 50 (residual activity $<22\%$), suggesting the presence of multiple nucleophilic binding-sites capable to interact with **1**. When **1**/r*Aae*UPO molar ratio was equal to 100, **1** retained some residual activity (51%, 1 h incubation time), whereas in the case of **1**/r*Aae*UPO molar ratios equal to 500, the regeneration catalyst was only slightly inhibited (residual activity $>80\%$, 1–5 h incubation time and 60% even after 24 h incubation time).

In a second set of experiments, the effect of varying **1** concentration on the activity of r*Aae*UPO in the ABTS assay[27] was explored. Results are shown in Figure 2b and Table S3. After one hour of incubation, no decrease of activity was observed for **1** to r*Aae*UPO ratio 50, whereas after 5 h (58%) and 24 h (21%) of incubation a greater inhibition was detected. This may indicate that some of the interacting amino acid residues of r*Aae*UPO are not surface-exposed. The coordination of easily accessible, surface-exposed amino acid residues to **1** is expected to be almost instantaneous while amino acids residing in more central parts of the biocatalyst are only sporadically accessible to the reaction medium (and thereby to **1**), therefore limiting the rate of the coordination reaction. Alternatively, protonation/deprotonation equilibria of basic amino acids may also play a role here. Increasing, **1** to r*Aae*UPO molar ratio to 100 the residual activity was drastically reduced (61%, 1 h incubation time; 14% 5 h incubation time) and completely inhibited at 500 **1**/r*Aae*UPO molar ratio. All these results point towards a mutual inhibition between **1** and r*Aae*UPO that critically depends on **1**/r*Aae*UPO molar ratio.

Based on the results illustrated in Figure 2, we decided to perform some oxyfunctionalisation experiments choosing firstly a **1**/r*Aae*UPO molar ratio of 25 as a compromise that has the drawback of causing a substantial decrease of the $FMNH_2$ regeneration activity of **1** but allows the performance of r*Aae*UPO to be mostly retained. Ethylbenzene was selected as well-known model substrate (Scheme 2),[28] under conditions where it is known to be converted into (*R*)-1-phenylethanol and subsequently overoxidised to acetophenone ([ethylbenzene] = 5 mM; [r*Aae*UPO] = 0.5 μM; buffer: 0.4 M NaPi pH 7 containing 5% v/v acetonitrile; [HCOONa] = 0.2 M; [FMN] = 0.1 mM; [**1**] = 12.5 μM; 298 K).[29] The reaction was followed by means of gas chromatography. The maximum alcohol production was reached after 4 hours, followed by overoxidation of (*R*)-1-phenylethanol to acetophenone as already observed (Figure 3a, Table S4). By means of linear trend fitting, it was possible to obtain an estimation of (*R*)-1-phenylethanol rate production of

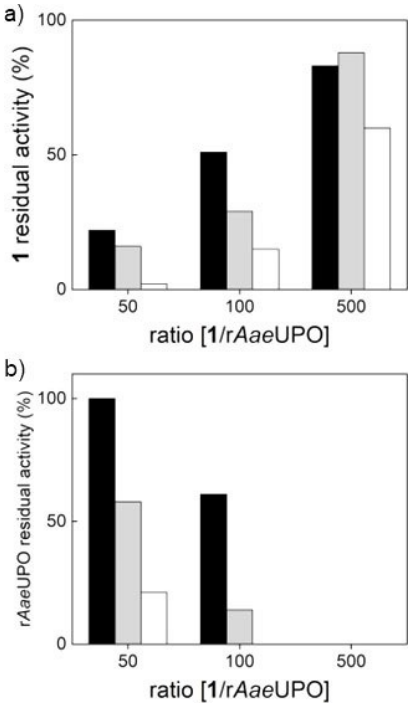

Figure 2. Residual activity of (a) **1** in the regeneration of $FMNH_2$ driven by HCOONa and (b) r*Aae*UPO in the ABTS assay, as a function of **1**/r*Aae*UPO molar ratio, at different incubation times (1 h, black; 5 h, grey; 24 h, white).

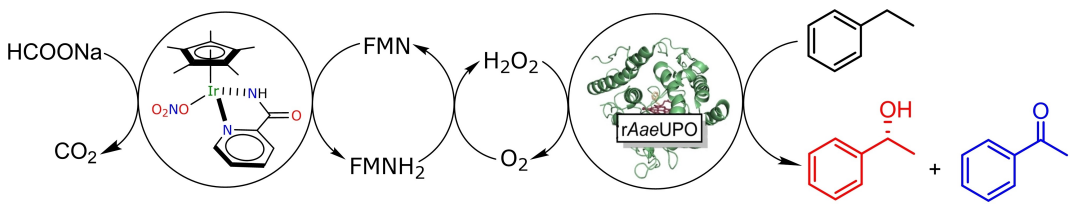

Scheme 2. Chemoenzymatic oxyfunctionalisation of ethylbenzene promoted by [Cp*Ir(pica)NO_3] and rAaeUPO catalytic tandem.

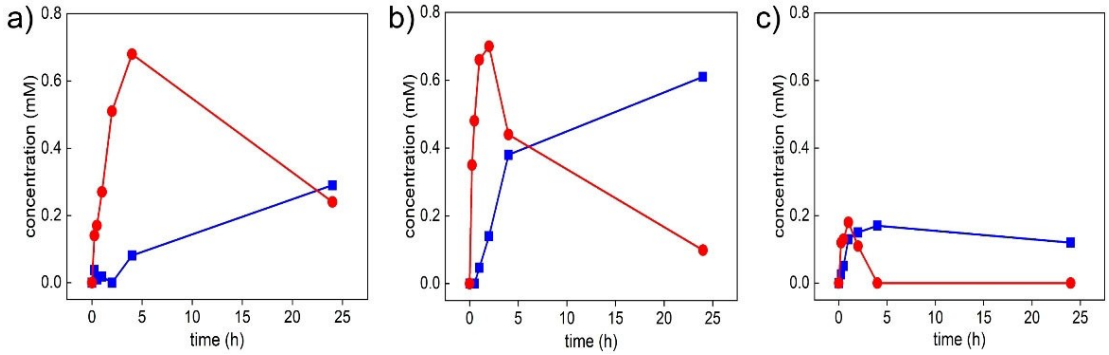

Figure 3. Time course of the (*R*)-1-phenylethanol (red dots) and acetophenone (blue squares) production from the oxidation of ethylbenzene promoted by **1** and r*Aae*UPO catalytic tandem. Reaction conditions: [ethylbenzene] = 5 mM; [r*Aae*UPO] = 0.5 μM; buffer: 0.4 M NaPi pH 7 containing 5% v/v acetonitrile; [HCOONa] = 0.2 M; [FMN] = 0.1 mM; [**1**] = 12.5 μM (a), 25 μM (b) and 50 μM (c); 298 K.

0.16 mM/h. Doubling the concentration of **1** up to 25 μM (Figure 3b–c, Table S4), with respect to that of the first trial experiment, led to approximately four times higher alcohol formation rate (0.61 mM/h), with the maximum (*R*)-1-phenylethanol production reached after 2 h; nevertheless, also in this case some overoxidation to the corresponding ketone was observed. At high concentration of **1** (100 μM), however, an intermediate formation rate (0.48 mM/h) was observed, but unfortunately the production of both (*R*)-1-phenylethanol and acetophenone stopped already after 2 h. Control experiments carried out under tandem reaction conditions except for the absence of **1** or r*Aae*UPO did not lead to any appreciable amount of product, clearly indicating that the system works synergistically only in tandem (Table S5, SI).

It must be noticed that ethylbenzene conversion was always rather low. This could be due to the presence of acetonitrile (ACN) as co-solvent. Since r*Aae*UPO activity is not impaired by ACN (up to 50% v/v),[29] we suspected **1** being inhibited by ACN. Indeed, a $FMNH_2$ regeneration test with **1** in the presence of 5% v/v acetonitrile (under otherwise the same experimental conditions than for the tandem reaction) exhibited no appreciable catalytic activity. A plausible explanation is that ACN competes with $HCOO^-$ for coordination to the metal centre and thereby impairs the FAD reduction reaction. In view of this control reaction, it is somewhat surprising that **1** showed some activity in the tandem system.

Identifying a non-coordinating cosolvent, which at the same time is not accepted by r*Aae*UPO as substrate will be a challenge for further optimisation of this reaction setup. However, also biphasic reaction media circumventing water-miscible cosolvents will be attractive for further, preparative-scale applications.

To improve the overall yield of the tandem reaction, we decided to perform an experiment at 50 **1**/r*Aae*UPO molar ratio, which appeared to be the optimal value, exploiting methanol as co-solvent instead of ACN ([ethylbenzene] = 20 mM; [r*Aae*UPO] = 1.0 μM; [**1**] = 50 μM; buffer: 0.4 M NaPi pH 7 containing 4% v/v methanol; [HCOONa] = 0.2 M; [FMN] = 4 mM; 303 K). After 24 h the starting material had been fully consumed and (*R*)-1-phenyl ethanol was obtained with > 99% *ee* (Table S6, entry 7). We therefore selected methanol as the co-solvent for exploring the scope of the chemoenzymatic system by testing some representative r*Aae*UPO substrates, at **1**/r*Aae*UPO molar ratio 50. All the reaction products were quantified by means of gas chromatography. As showed in Table 1, ethylbenzene derivatives **a**–**c** were successfully converted into the corresponding alcohol and ketone products. Higher conversion was observed for **a** (TON = 18933) followed by **c** (TON = 15702) and **b** (TON = 8913). For both **a** and **c** the overoxidation to the corresponding ketone was quite low (ca 10%), whereas for **b** it amounted at 50%. In all cases, only the (*R*)-alcohol formation was observed indicating that the oxyfunctionalisation of the substrates was r*Aae*UPO-catalysed and the regeneration catalyst **1** and the enzyme work synergistically in tandem. **1**/r*Aae*UPO was able to promote the epoxidation of **d** (TON = 13488), leading exclusively (1*R*,2*S*)-cis-methyl styrene oxide, demonstrating the applicability of the *in situ* H_2O_2 regeneration system also for epoxidation reaction.

Cyclohexane and thioanisole were also oxidised by **1**/r*Aae*UPO tandem but with modest performance (Table 1). The observed low conversion (TON < 2000) might be due to substrate evaporation in case of the volatile cyclohexane and inhibition of **1** in case of thoanisol.

Generally speaking, a maximum TON of 18933 (Table 1, substrate **a**) has been observed for r*Aae*UPO/**1** tandem-catalysed oxyfunctionalisation of ethylbenzene, which corresponds to roughly 45 $g_{prod} \cdot g_{AaeUPO}^{-1}$. The TOF referred to the moles of **1** was in the range of 380 h^{-1} and the total turnover number (TTON), which is defined as product mole per cofactor mole, was 4.8 that is in line with the values previously reported for Rh@PMO in combination with horse liver alcohol dehydrogenase (HLADH),[30] indicating that H_2O_2 is catalytically generated in the combined reaction system.

Conclusion

The potentiality of integrating organometallic and enzymatic catalysis has been herein demonstrated. The hybrid catalytic system comprising [Cp*Ir(pica)NO_3] **1**, to regenerate $FMNH_2$

Table 1. Oxyfunctionalisation of substrates **a**–**f** by **1** and r*Aae*UPO catalytic tandem.[a]

Substrate	Product 1 (mM)	Product 2 (mM)	ee [%]	TON_{AaeUPO}
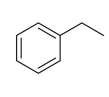	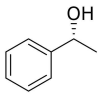	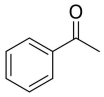		
a	16 ± 0.3	3.1 ± 0.05	> 99 (*R*)	18933 ± 337
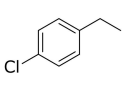	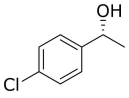	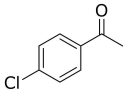		
b	4.6 ± 0.1	4.3 ± 0.08	> 99 (*R*)	8913 ± 232
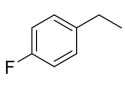	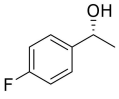	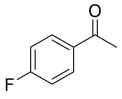		
c	12 ± 0.5	4.0 ± 0.1	> 99 (*R*)	15702 ± 699
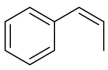	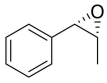	–	> 99 (1*R*, 2*S*)	13488 ± 754
d	13 ± 0.7			
	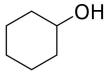		n.d.	1634 ± 516
e	1.6 ± 0.5	0.04 ± 0.1		
	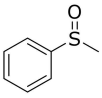	–	n.d.	1369 ± 136
f	1.4			

[a] Experimental conditions: pH 7 by 0.4 M NaPi buffer containing 4% v/v MeOH; [HCOONa] = 0.2 M; [substrate] = 20 mM; [r*Aae*UPO] = 1.0 μM; [1] = 50 μM; [FMN] = 4 mM for **a** and **c** substrates, 1 mM for substrate **b**, **d**–**f**; T = 303 K. Data are expressed as the mean ± SD of the two independent experiments performed in technical duplicates.

from NaHCOO, and r*Aae*UPO, which, taking advantage of H_2O_2 provided by the spontaneous reaction of formed $FMNH_2$ and O_2, catalyses oxyfunctionalisation reactions, represents a proof-of-concept of the complementarity and synergistic effects of the two types of catalysis. At the same time, the results reported in this paper show that it is essential to conduct an in-depth optimisation study to understand under what conditions the two catalytic systems can work efficiently while minimising relative inhibitions. In this regard, it is reasonable to assume that immobilisation of one or both catalytic components can resolve or drastically mitigate their mutual inhibition by physical separation.[25b] Studies in this direction are ongoing in our laboratories. Envisioning preparative-scale application of the proposed reaction system will also necessitate reaction engineering to increase the overall substrate and product payload. Water-miscible cosolvents such as ACN used here do not appear suitable due to inhibitory effects. Future studies will rather concentrate on two liquid phase systems comprising the hydrophobic starting material as substrate reservoir and product sink.

Experimental Section

Enzyme preparation: Recombinant expression and preparation of the evolved unspecific peroxygenase from *A. aegerita* r*Aae*UPO (PaDa-I mutant) in *P. pastoris* were performed following a previously described procedure.[27] The enzyme preparation used had a Reinheitszahl (Rz-value A_{418}/A_{280}) of 0.6 and an UPO-concentration of 56 μM after one step of purification[6a] (Supporting information Figure S3). 20 mM phosphate buffer (pH 7) was used for storage of the enzyme at −20 °C.

FMN reduction: The reaction was monitored by UV-Vis spectroscopy, following the depletion of the absorption band of FMN centred at 455 nm ($\varepsilon = 10000\ M^{-1}cm^{-1}$), using a Cary 60 UV VIS spectrophotometer (Agilent). In a typical experiment, 1 mL of a solution of FMN (0.1 mM in phosphate buffer (pH = 7, 0.4 M)) were transferred inside a cuvette. The system was allowed to equilibrate under stirring for 5 min at 298 K in N_2 atmosphere. After background correction, 15–30 μL of a solution of the catalyst was injected and data acquisition started. Turnover frequency [TOF = moles of $FMNH_2$/(moles of catalyst *per* unit time)] values were obtained by deriving the TON *versus* t linear trends in the first 5% of reaction progress.

Inactivation of 1 by r*Aae*UPO: **1** (20 μM) was incubated in the presence of r*Aae*UPO (0.2–0.04 μM) in phosphate buffer at 25 °C. After 1, 5 and 24 h the mixtures were supplemented with FMN and analysed spectrophotometrically. Prior to the assay, the sample was equilibrated at the desired temperature under nitrogen for at least 2 minutes. The reaction was started by addition of formate. The values of turnover frequency were derived as above. Then, **1** residual activity is calculated as the ratio TOF/TOF_0, where $TOF_0 = 350\ h^{-1}$.

Inactivation of r*Aae*UPO by 1: r*Aae*UPO (0.5 μM) was incubated in phosphate buffer (0.4 M, pH 7) at 298 K with **1** (0–250 μM). After 1,

5 and 24 h the peroxidase activity of r*Aae*UPO was determined in a continuous photometric assay against the substrate 2,2′-azino-bis(3-ethylbenzothiazoline-6-sulfonic acid (ABTS) at 420 nm (ε_{420} = 36.0 $mM^{-1}cm^{-1}$). The incubation mixture was supplemented with 0.5 mM ABTS in 2 mL plastic cuvettes. After short incubation at 298 K, measurements were started by addition of 2 mM H_2O_2. The increase of absorption at 420 nm caused by ABTS formation was tracked spectrophotometrically. The initial slope (ΔA_{420}/min) between 20–80 s was linear and thus used to calculate the volumetric activity [U/mL]. Then, r*Aae*UPO residual activity is calculated as the ratio (U/mL)/$(U/mL)_0$, where $(U/mL)_0$ = 21.8 μM $ABTSmin^{-1}mL^{-1}$.

Chemoenzymatic oxyfunctionalisation of ethylbenzene: The reactions were performed in 2.0 mL glass vials placed in a thermomixer containing a solution of sodium phosphate buffer (0.4 M at pH 7) and 0.2 M sodium formate previously bubbled with air. After supplementation with r*Aae*UPO, FMN and ethyl benzene (10 μL substrate in co-solvent), 250 μL of reaction mixture was maintained at 298 K for some minutes. The reactions were started by the addition of **1** and incubated at 600 rpm in an Eppendorf shaker. Reactions were stopped by the addition of 250 μL of n-heptane containing 5 mM n-octanol as internal standard with subsequent mixing. The product was extracted twice, and the obtained supernatant was analysed by GC-FID.

Substrate scope: The screening was performed in 0.4 M sodium phosphate buffer containing 0.2 M sodium formate at pH 7 in 2.0 mL glass vial. After supplementation with r*Aae*UPO, FMN and substrate (10 μL methanol as co-solvent), 250 μL of reaction mixture was maintained at 303 K for some minutes. The reactions were started by the addition of **1** and incubated at 600 rpm in an Eppendorf shaker. Reactions were terminated by the addition and subsequent mixing of 250 μL of n-heptane or ethylacetate containing 5 mM n-octanol as internal standard. The reaction mixtures were extracted twice with the respective organic solvents and the obtained supernatant was analysed by GC-FID.

Acknowledgements

Funded by the European Union (ERC, PeroxyZyme, No 101054658). Views and opinions expressed are however those of the authors only and do not necessarily reflect those of the European Union or the European Research Council. Neither the European Union nor the granting authority can be held responsible for them. C. D. thanks Erasmus+Traineeship program (KA1-2020-1-IT02-KA103-078486). C. D. and A. M. acknowledge the University of Perugia and MIUR (AMIS, "Dipartimenti di Eccellenza-2018–2022" program) for the financial support.

Conflict of Interest

The authors declare no conflict of interest.

Data Availability Statement

The data that support the findings of this study are available in the supplementary material of this article.

Keywords: chemoenzymatic tandem · FMN reduction · iridium · oxyfunctionalisation · peroxygenases

[1] J. Dong, E. Fernández-Fueyo, F. Hollmann, C. Paul, M. Pesic, S. Schmidt, Y. Wang, S. Younes, W. Zhang, *Angew. Chem.* **2018**, *130*, 9380–9404, *Angew. Chem. Int. Ed.* **2018**, *57*, 9238–9261.
[2] V. B. Urlacher, M. Girhard, *Trends Biotechnol.* **2019**, *37*, 882–897.
[3] D. Holtmann, F. Hollmann, *ChemBioChem* **2016**, *17*, 1391–1398.
[4] M. Hobisch, D. Holtmann, P. G. de Santos, M. Alcalde, F. Hollmann, S. Kara, *Biotechnol. Adv.* **2021**, *51*, 107615.
[5] R. Ullrich, J. Nüske, K. Scheibner, J. Spantzel, M. Hofrichter, *Appl. Environ. Microbiol.* **2004**, *70*, 4575–4581.
[6] a) P. Molina-Espeja, E. Garcia-Ruiz, D. Gonzalez-Perez, R. Ullrich, M. Hofrichter, M. Alcalde, *Appl. Environ. Microbiol.* **2014**, *80*, 3496–3507; b) P. Molina-Espeja, S. Ma, D. M. Mate, R. Ludwig, M. Alcalde, *Enz. Microb. Technol.* **2015**, *73–74*, 29–33.
[7] B. Valderrama, M. Ayala, R. Vazquez-Duhalt, *Chem. Biol.* **2002**, *9*, 555–565.
[8] B. O. O. Burek, S. Bormann, F. Hollmann, J. Bloh, D. Holtmann, *Green Chem.* **2019**, *21*, 3232–3249.
[9] a) F. Tieves, S. J.-P. Willot, M. M. C. H. van Schie, M. C. R. Rauch, S. H. H. Younes, W. Zhang, P. G. de Santos, J. M. Robbins, B. Bommarius, M. Alcalde, A. Bommarius, F. Hollmann, *Angew. Chem.* **2019**, *131*, 7955–7959, *Angew. Chem. Int. Ed.* **2019**, *58*, 7873–7877; b) Y. Ni, E. Fernández-Fueyo, A. G. Baraibar, R. Ullrich, M. Hofrichter, H. Yanase, M. Alcalde, W. J. H. van Berkel, F. Hollmann, *Angew. Chem.* **2016**, *128*, 809–812, *Angew. Chem. Int. Ed.* **2016**, *55*, 798–801; c) J. Rocha-Martin, S. Velasco-Lozano, J. M. Guisan, F. Lopez-Gallego, *Green Chem.* **2014**, *16*, 303–311; d) Y. R. Li, Y. J. Ma, P. L. Li, X. Z. Zhang, D. Ribitsch, M. Alcalde, F. Hollmann, Y. H. Wang, *ChemPlusChem* **2020**, *85*, 254–257; e) P. G. de Santos, S. Lazaro, J. Viña-Gonzalez, M. D. Hoang, I. Sánchez-Moreno, A. Glieder, F. Hollmann, M. Alcalde, *ACS Catal.* **2020**, *10*, 13524–13534; f) A. Al-Shameri, S. J. P. Willot, C. E. Paul, F. Hollmann, L. Lauterbach, *Chem. Commun.* **2020**, *56*, 9667–9670.
[10] a) C. H. Yun, J. Kim, F. Hollmann, C. B. Park, *Chem. Sci.* **2022**, *13*, 12260–12279; b) M. Mifsud, S. Gargiulo, S. Iborra, I. W. C. E. Arends, F. Hollmann, A. Corma, *Nat. Commun.* **2014**, *5*, 3145 ; c) E. Churakova, M. Kluge, R. Ullrich, I. Arends, M. Hofrichter, F. Hollmann, *Angew. Chem.* **2011**, *123*, 10904–10907, *Angew. Chem. Int. Ed.* **2011**, *50*, 10716–10719; d) D. I. Perez, M. Mifsud Grau, I. W. C. E. Arends, F. Hollmann, *Chem. Commun.* **2009**, *44*, 6848–6850.
[11] a) C. Kohlmann, S. Lütz, *Eng. Life Sci.* **2006**, *6*, 170–174; b) S. Bormann, M. van Schie, T. P. De Almeida, W. Y. Zhang, M. Stockl, R. Ulber, F. Hollmann, D. Holtmann, *ChemSusChem* **2019**, *12*, 4759–4763; c) L. Getrey, T. Krieg, F. Hollmann, J. Schrader, D. Holtmann, *Green Chem.* **2014**, *16*, 1104–1108; d) T. Krieg, S. Huttmann, K.-M. Mangold, J. Schrader, D. Holtmann, *Green Chem.* **2011**, *13*, 2686–2689; e) A. E. W. Horst, S. Bormann, J. Meyer, M. Steinhagen, R. Ludwig, A. Drews, M. Ansorge-Schumacher, D. Holtmann, *J. Mol. Catal. B* **2016**, *133*, S137–S142.
[12] a) S. J. Freakley, S. Kochius, J. van Marwijk, C. Fenner, R. J. Lewis, K. Baldenius, S. S. Marais, D. J. Opperman, S. T. L. Harrison, M. Alcalde, M. S. Smit, G. J. Hutchings, *Nat. Commun.* **2019**, *10*, 4178; b) F. Hollmann, A. Schmid, *J. Inorg. Biochem.* **2009**, *103*, 313–315.
[13] a) J. Yoon, H. Jang, M.-W. Oh, T. Hilberath, F. Hollmann, Y. S. Jung, C. B. Park, *Nat. Commun.* **2022**, *13*, 3741; b) J. Kim, T. V. T. Nguyen, Y. H. Kim, F. Hollmann, C. B. Park, *Nat. Synth.* **2022**, *1*, 217–226; c) J. Kim, J. Jang, T. Hilberath, F. Hollmann, C. B. Park, *Nat. Synth.* **2022**, *1*, 776–786; d) W. Zhang, H. Liu, M. M. C. H. van Schie, P.-L. Hagedoorn, M. Alcalde, A. G. Denkova, K. Djanashvili, F. Hollmann, *ACS Catal.* **2020**, *10*, 14195–14200; e) J. Yoon, J. Kim, F. Tieves, W. Y. Zhang, M. Alcalde, F. Hollmann, C. B. Park, *ACS Catal.* **2020**, *10*, 5236–5242; f) A. Yayci, A. G. Baraibar, M. Krewing, E. F. Fueyo, F. Hollmann, M. Alcalde, R. Kourist, J. E. Bandow, *ChemSusChem* **2020**, *13*, 2072–2079.
[14] a) R. Kanega, N. Onishi, S. Tanaka, H. Kishimoto, Y. Himeda, *J. Am. Chem. Soc.* **2021**, *143*, 1570–1576; b) A. Nijamudheen, R. Kanega, N. Onishi, Y. Himeda, E. Fujita, M. Z. Ertem, *ACS Catal.* **2021**, *11*, 5776–5788; c) R. Kanega, N. Onishi, L. Wang, Y. Himeda, *ACS Catal.* **2018**, *8*, 11296–11301; d) L. Tensi, A. V. Yakimov, C. Trotta, C. Domestici, J. De Jesus Silva, S. R. Docherty, C. Zuccaccia, C. Copéret, A. Macchioni, *Inorg. Chem.* **2022**, *61*, 10575–10586.

[15] a) A. Bucci, S. Dunn, G. Bellachioma, G. Menendez Rodriguez, C. Zuccaccia, C. Nervi, A. Macchioni, *ACS Catal.* **2017**, *11*, 7788–7796; b) L. Tensi, A. Macchioni, *ACS Catal.* **2020**, *10*, 7945–7949.
[16] R. Kanega, N. Onishi, D. J. Szalda, M. Z. Ertem, J. T. Muckerman, E. Fujita, Y. Himeda, *ACS Catal.* **2017**, *7*, 6426–6429.
[17] a) A. H. Ngo, M. Ibañez, L. H. Do, *ACS Catal.* **2016**, *6*, 2637–2641; b) S. Bose, A. H. Ngo, L. H. Do, *J. Am. Chem. Soc.* **2017**, *139*, 8792–8795.
[18] a) R. Kanega, N. Onishi, L. Wang, K. Murata, J. T. Muckerman, E. Fujita, Y. Himeda, *Chem. Eur. J.* **2018**, *24*, 18389–18392; b) G. Menendez Rodriguez, C. Domestici, A. Bucci, M. Valentini, C. Zuccaccia, A. Macchioni, *Eur. J. Inorg. Chem.* **2018**, *2018*, 2247–2250; c) G. Menendez Rodriguez, F. Zaccaria, L. Tensi, C. Zuccaccia, P. Belanzoni, A. Macchioni, *Chem. Eur. J.* **2021**, *27*, 2050–2064.
[19] a) M. Watanabe, J. Hori, K. Murata, *EP 2228377* **2010**; b) C. K. Hill, J. F. Hartwig, *Nat. Chem.* **2017**, *9*, 1213–1221; c) K. Tanaka, T. Miki, K. Murata, A. Yamaguchi, Y. Kayaki, S. Kuwata, T. Ikariya, M. Watanabe, *J. Org. Chem.* **2019**, *84*, 10962–10977; d) D. P. Nguyen, R. N. Sladek, L. H. Do, *Tet. Lett.* **2020**, *61*, 152196.
[20] T. Beppu, K. Sakamoto, Y. Nakajima, K. Matsumoto, K. Sato, S. Shimada, *J. Organomet. Chem.* **2018**, *869*, 75–80.
[21] H. T. H. Nguyen, L. H. Do, *Chem. Commun.* **2020**, *56*, 13381–13384.
[22] a) T. J. Kotzé, S. Duffy, V. M. Avery, A. Jordaan, D. F. Warner, L. Loots, G. S. Smith, P. Chellan, *Inorg. Chim. Acta* **2021**, *517*, 120175; b) Z. Almodares, S. J. Lucas, B. D. Crossley, A. M. Basri, C. M. Pask, A. J. Hebden, R. M. Phillips, P. C. McGowan, *Inorg. Chem.* **2014**, *53*, 727–736; c) N. R. Palepu, J. Richard Premkumar, A. K. Verma, K. Bhattacharjee, S. R. Joshi, S. Forbes, Y. Mozharivskyj, K. Mohan Rao, *Arab. J. Chem.* **2018**, *11*, 714–728; d) S. J. Lucas, R. M. Lord, A. M. Basri, S. J. Allison, R. M. Phillips, A. J. Blacker, P. C. McGowan, *Dalton Trans.* **2016**, *45*, 6812–6815.
[23] F. Hollmann, B. Witholt, A. Schmid, *J. Mol. Catal. B* **2002**, *19–20*, 167–176.
[24] S. Shibata, T. Suenobu, S. Fukuzumi, *Angew. Chem.* **2013**, *125*, 12553–12557, *Angew. Chem. Int. Ed.* **2013**, *52*, 12327–12331.
[25] a) M. Poizat, I. W. C. E. Arends, F. Hollmann, *J. Mol. Catal. B. Enzym.* **2010**, *63*, 149–156; b) F. Hildebrand, S. Lütz, *Chem. Eur. J.* **2009**, *15*, 4998–5001.
[26] F. E. H. Nintzel, Y. Wu, M. Planchestainer, M. Held, M. Alcalde, F. Hollmann, *Chem. Commun.* **2021**, *57*, 5766–5769.
[27] F. Tonin, F. Tieves, S. Willot, A. van Troost, R. van Oosten, S. Breestraat, S. van Pelt, M. Alcalde, F. Hollmann, *Org. Process Res. Dev.* **2021**, *25*, 1414–1418.
[28] M. Kluge, R. Ullrich, K. Scheibner, M. Hofrichter, *Green Chem.* **2012**, *14*, 440–446.
[29] T. Hilberath, A. van Troost, M. Alcalde, F. Hollmann, *Frontiers in Catalysis* **2022**, *2*, 882992 .
[30] T. Himiyama, M. Waki, Y. Maegawa, S. Inagaki, *Angew. Chem.* **2019**, *131*, 9248–9252, *Angew. Chem. Int. Ed.* **2019**, *58*, 9150–9154.

Manuscript received: December 19, 2022
Revised manuscript received: March 8, 2023
Accepted manuscript online: March 8, 2023
Version of record online: March 24, 2023